10th Annual CFD Symposium 11th – 12th August 2008

Numerical Simulation of Supersonic Combustion in a Slant Cavity

Ashfaque A. Khan and T.R.Shembharkar
Propulsion Division, National Aerospace Laboratories, Bangalore –560 017
(Council for Scientific & Industrial Research, India)

ABSTRACT

A commercial CFD code has been used to compute supersonic combustion in a slant cavity with upstream fuel injection. The 2-D steady state Reynolds Averaged Navier-Stokes equations along with RNG k-ε turbulence model have been solved. Combustion has been modeled by a 5-step 7-species reaction mechanism. The pressure-based algorithm, which the code uses, requires quite some adjustment of solution controlling options and boundary conditions for obtaining the solution. Experiences of using such algorithm for high speed flows are discussed in the paper. The converged solution, however, predicts the important flow features like separation shock ahead of fuel injection, bow shock near fuel injection, free shear layer across the cavity, flow recirculation inside the cavity, impingement of shear layer on slant wall and oblique shock at the trailing edge reasonably well.

KEYWORDS: CFD, slant cavity, supersonic combustion, multi-step reaction, pressure-based algorithm

1. INTRODUCTION

During the last few years, cavities have gained the attention of high-speed combustion researchers as a promising integrated fuel injection/flame holding device. The main idea is to create a recirculation region inside the cavity with a pool of radicals which will facilitate the ignition of fuel/air mixture on a sustained basis and stabilize the flame. There have been some excellent review papers [1,2] on the aspects of high-speed flow behaviour over the cavity. In general, the boundary layer ahead of the cavity separates at the leading edge of the cavity forming a free shear layer, which reattaches at some other point downstream. The reattachment point depends upon the geometry of the cavity and the external flow conditions. If the reattachment takes place at the back face of the cavity, the cavity is called "open" cavity but if it takes place on the lower wall, the cavity is called "closed" cavity. The open cavities have aspect ratio less than about 7-10 while the closed cavity have higher aspect ratios. Flow recirculation takes place inside the cavity. Depending upon the pressure inside the cavity, the separated free shear layer may be locally deflected upwards or downwards producing a shock wave or an expansion wave at the leading edge while a strong shock generally exist at the trailing edge. The leading edge shock, flow separation, recirculation, reattachment of free shear layer and trailing edge shock contribute to the pressure loss in the cavity.

Address for correspondence:
Ashfaque A. Khan, Propulsion Division, National Aerospace Laboratories, Bangalore-560017.
Phone: +91-80-25051605, Fax: +91-80-25222494 Email: ashfaque@css.nal.res.in

In general, a cavity exposed to a supersonic flow stream experiences self sustained oscillations which can induce fluctuating pressures, densities and velocities. These are essentially caused by the unsteady

motion of the free shear layer above the cavity. In open cavities, the oscillation propagation is in transverse mode in low aspect ratio configuration and in longitudinal mode in higher aspect ratio configuration. In recent times, considerable research effort is being directed towards making use of these cavity oscillations for increasing mixing in supersonic shear layer and improving the performance of the cavity. However, the high-pressure loss and noise generation associated with this technique have to be understood more thoroughly. On the other hand, it is possible to control the oscillations by proper design of cavity or by a passive/active control system in order to obtain stable combustion. One of the passive methods is use of slant back wall, which modifies the shear layer so that the reattachment process does not reflect the pressure waves into the cavity while one of the active control methods is fluid injection at the leading edge of the cavity, which may thicken the shear layer and alter its instability characteristics. Combining these two schemes, a slant cavity with upstream normal fuel injection is one of the possible cavity flame holder configuration.

There have been several experimental investigations [3-5] to understand the basic flow features in slant cavity without combustion in the past. A great amount of understanding of the flow phenomenon has resulted from such experimental studies. Numerical investigations [6-8] have also looked into the reactive flow over the slant cavity with different fuel injection configurations. These computations have generally been carried out employing density-based algorithm along with combustion model of different complexities. The present paper is aimed at computing the steady state supersonic flow in a 2-D slant cavity with an upstream fuel injection with the help of a pressure-based algorithm and a multi-step reaction model. In the present scenario, many commercial CFD codes are becoming popular and are increasingly used to solve engineering problems. We have access to one such code called CFD-ACE+, which is based on a pressure-based algorithm, namely SIMPLEC. In order to explore the applicability of this algorithm in high-speed flows, we carried out the flow computation with this code. The predicted flow features are described in the paper.

2. NUMERICAL APPROACH

Figure 1 shows the configuration of slant cavity with upstream fuel injection. It has an aspect ratio (L/D) of 3 and the aft angle of 30 degrees [7]. The depth of the cavity D is equal to 15mm. The fuel injection passage is 1mm wide and situated at 7.5 mm upstream from front face of the cavity. The inlet boundary is 40mm upstream and the outlet boundary 120mm downstream from the front face of cavity. The top boundary of the computational domain is located at 60mm above the cavity. The figure also shows the multi-block grid adopted for the computations. The grid density was kept high in the vicinity of wall, fuel injection and free shear layer. Total number of grid cells in the computational domain is 16671.

2.1 Governing equations

The general form of the governing RANS equations is given by,

$$\frac{\partial(\rho\phi)}{\partial t} + \nabla \bullet (\rho\overline{V}\phi) = \nabla \bullet (\Gamma_\phi \nabla\phi) + S_\phi$$

Where the general variable ϕ stands for the dependent variables, namely 1 in continuity equation, Cartesian velocity components U, V, W in three momentum equations, total enthalpy H in energy equation, species mass fraction m_i in species transport equations, turbulent kinetic energy k and dissipation rate ε in turbulence model. The other variables ρ, $\overline{V}$ and Γ_ϕ are density, velocity vector and diffusion coefficient for ϕ. The source term S_ϕ stands for all the terms not included in transient, convection or diffusion terms in transport equation of ϕ.

2.2 Turbulence model

The RNG k-ε turbulence model has been used in the computation. It is a variation of the standard k-ε turbulence model. It has same transport equations for k and ε but the model coefficients take different values [8],

C_μ = 0.085, C_{ε_2} = 1.68 and $\sigma_k = \sigma_\varepsilon$ = 0.7179

Like standard k-ε model, it is a high Reynolds number model and wall functions are used at the wall boundaries.

2.3 Combustion model

The present combustion model assumes 5-step 7-species finite rate reactions for the Hydrogen-Air system. The conservation equations are solved for each of the species mass fraction with appropriate source term. The reaction steps are given in Table 1.

Table 1: Reaction steps

Reaction	A_i	n_i	E_a/R_i	m_i
$H_2 + O_2 \rightarrow 2OH$	1.0×10^9	0.0	4.69	0.0
$OH + H_2 \rightarrow H_2O + H$	6.31×10^{10}	0.0	0.71	0.0
$H + O_2 \rightarrow OH + O$	2.2×10^{11}	0.0	1.98	0.0
$O + H_2 \rightarrow OH + H$	1.1×10^{10}	0.0	1.13	0.0
$H + OH + M \rightarrow H_2O + M$	1.0×10^{11}	0.0	0.0	0.0

Here, M: Third Body and Reaction Rate Constant $K_i = A_i T^n \left(\frac{p}{p_{atm}}\right)^m e^{\left(-E_a/RT\right)}$

2.4 Numerical algorithm [9]

The present computations have been done with a pressure-based method (SIMPLEC algorithm) on a body-fitted structured grid. It is a cell centered finite volume approach. All the dependent and auxiliary variables are stored at the cell center. The convective terms are discretized by a hybrid upwind-central blended scheme (blending factor = 0.9) and the diffusion terms by central difference scheme. An iterative segregated solution method is employed, wherein the equation sets for each variable are solved sequentially and repeatedly by conjugate gradient squared linear solver until a converged solution is obtained. The dependent variables are under-relaxed by inertial under-relaxation (false time-step) and the auxiliary variables by linear under-relaxation to ensure overall convergence.

3. BOUNDARY CONDITIONS

The inlet conditions for which the computations have been done are [7]

Free-stream conditions:

Mach number = 2.5

Static pressure = 1 atm

Temperature = 1000 K

Fuel injection conditions

Mach number = 1.0

Stagnation pressure = 7.57 atm

Stagnation temperature = 600 K

The relevant velocities, pressure and density at the air inlet and fuel inlet were derived from the above conditions. All the bottom walls of the cavity were specified no-slip wall condition. The upper boundary was given symmetry condition. The exit boundary conditions were satisfied by extrapolating the corresponding variables from inside.

4. RESULTS AND DISCUSSION

Computations were done for the specific boundary condition mentioned above. It was realized that getting a converged solution from the commercial code was not a straightforward task. The pressure-based algorithm does not yield highly compressible flow solutions readily. For convective terms, various options regarding difference scheme were tried. The hybrid upwind-central blended scheme only ensured convergence. The inlet conditions in terms of inlet total pressure and temperature failed to yield convergence. They were changed to inlet velocity and density conditions, which essentially fixed the mass flow at the inlet. Three different combustion models were tried; only the 5-step reaction model gave sensible results. Hence, the final converged solution was obtained with hybrid scheme for convective terms, fixed velocity condition for inlet boundary and 5-step reaction model for combustion. It is this solution which will be discussed below. The reasons for failure to obtain meaningful converged solutions for other options would be explored in future work.

Figure 2 shows the contour plots of Mach number. It also shows the velocity vector plot and streamline plot inside the cavity, and streamline plot near the fuel injection. The separation shock ahead of the fuel injection, bow shock near the fuel injection slot, appearance of free shear layer across the cavity, impingement of shear layer on the inclined wall and the trailing edge shock are clearly visible in the figure 2(a). The Mach number is low inside the cavity. The stable recirculating flow in this region can be observed in the velocity vector plot in Figure 2(b) and the streamline plot in Figure 2(c). The small separation zone ahead of the fuel injection is visible in the streamline plot in Figure 2(d). The Mach number plot shown in Figure 2(a) can be compared with the similar plot of Reference [7] reproduced here in Figure 7(a). There is good qualitative agreement between the two results.

Figure 3 shows the pressure contour plot. The increase of pressure across the shocks along with nearly uniform pressure inside most of the cavity region is seen in the figure. The pressure inside the cavity is slightly lower than the free stream pressure, which causes the free shear layer to deflect downwards towards the cavity. There is reasonable qualitative agreement between the present prediction and that of Reference [7] reproduced in Figure 7(b).

Figure 4 shows the contour plots of temperature and fuel concentration (H2). The high temperatures are observed inside the cavity in Figure 4(a). The rise in temperature in the vicinity of fuel injection indicates that the combustion takes place in this region. The temperature rises across the shocks. The low temperature along the wall behind fuel injection is due to lower fuel temperature. The contour plot for H2 in Figure 4(b) indicates that the fuel is consumed entirely in the vicinity of the fuel injection. The recirculating flow in the

cavity is at relatively high temperature. The predicted temperature plot shows qualitative agreement with the result of Reference [7] reproduced in Figure 7(c).

The flow on the slant wall is quite complex due to the interaction between the boundary layer, free shear layer and shock wave. The velocity and pressure profiles in the normal direction at different stations of the slant wall are shown in Figure 5. The velocity is normalized with local free-stream velocity and the pressure is normalized with the inlet pressure. The stations are identified from their distances from inlet in this figure. Figure 5(a) indicates little back flow on a part of the slant wall before more conventional boundary layer is realized on the wall. The pressure profiles are more complex at the same stations as seen in Figure 5(b).

Figure 6 shows the variation of pressure, Mach number, temperature across the exit. Pressure profile shows considerable variation across the height while Mach number and temperature profiles are relatively uniform for most of the exit height.

5. CONCLUSIONS

A commercial CFD code based on pressure-based algorithm has been used to compute supersonic flow over a slant cavity with upstream fuel injection. Experience shows that the pressure-based algorithm though excellent for low Mach number flows does not work very efficiently for high Mach number flows. Solution could be obtained for the supersonic flow but it required quite some adjustment of solution controlling parameters and boundary conditions. The converged solution, however, predicts the important flow features like separation shock, separation zone and bow shock near fuel injection, free shear layer across the cavity, recirculation inside the cavity, impingement of shear layer on slant wall and the trailing edge shock reasonably well.

ACKNOWLEDGEMENTS

The authors thank the CSIR Centre for Mathematical modelling and Computer Simulation (C-MMACS), Bangalore for providing the computing facilities

REFERENCES

[1] Adela Ben-Yakar and Ronald K. Hanson, ‘Cavity flame-holders for ignition and flame stabilization in scramjets: An overview’, Journal of Propulsion and Power, 17(4), 869-877, 2001.

[2] Adela Ben-Yakar and Ronald K. Hanson, ‘Cavity flame-holders for ignition and flame stabilization in scramjets: Review and experimental study’, AIAA-98-3122, 1998.

[3] M.Samimy, H.L.Petrie and A.L.Addy, ‘A study of compressible turbulent reattaching free shear layers’, AiAA Journal 24(2), 261-267, 1986

[4] M.R.Gruber, R.A.Baurle, T.Mathur and K.-Y.Hsu, ‘Fundamental studies of cavity-based flameholder concepts for supersonic combustors’, Journal of Propulsion and Power 17(1), 146-153, 2001.

[5] Ken H.Yu, Ken J.Wilson and Klaus C.Schadow, ‘Effect of flame-holding cavities on supersonic-combustion performance’, Journal of Propulsion and Power, 17(6), 1287-1295, 2001.

[6] D.L.Davis and R.D.W.Bowersox, ‘Computational fluid dynamics analysis of cavity flame holders for scramjets’, AIAA-97-3270, 1997.

[7] K.M.Kim, S.W.Baek and C.Y.Han, ‘Numerical study on supersonic combustion with cavity-based fuel injection’, Int. Journal of Heat and Mass Transfer, 47, 271-286, 2004.

[8] C.K.Kim, S.-T.John Yu and Z.C.Zhang, ‘Cavity flow in scramjet engine by space-time conservation and solution element method’, AIAA Journal, 42(5), 912-919, 2004.

[9] CFD-ACE+ 2003 user’s manual, CFD Research Corporation, USA

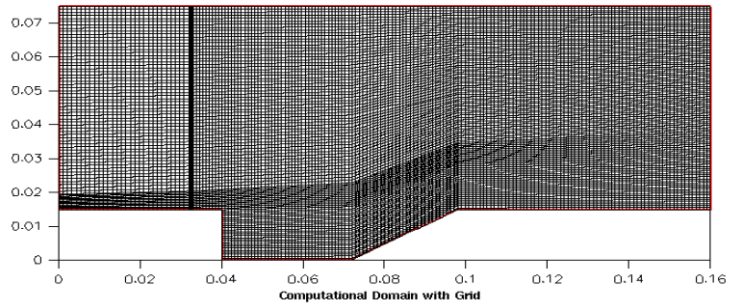

Figure 1. Computational Domain with Grid

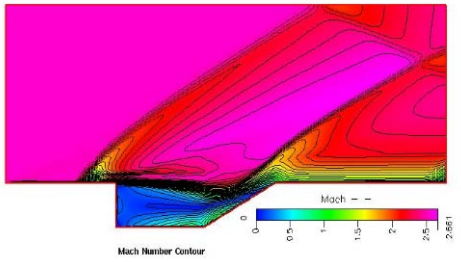

(a) Mach number

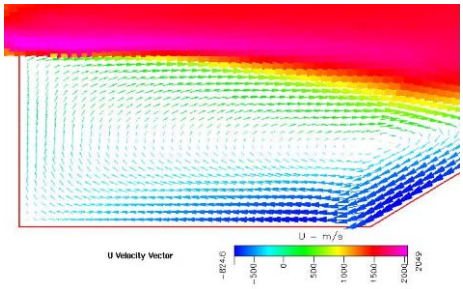

(b) Velocity Vector

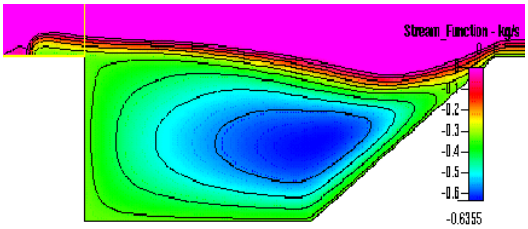

(c) Streamline plot inside the cavity

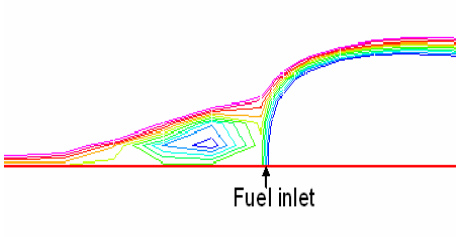

(d) Streamline plot near fuel injection

Figure 2. Mach Number, Velocity vector and Streamline plots

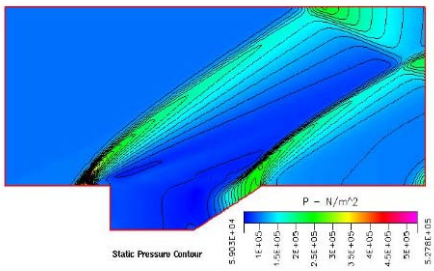

Figure 3. Static pressure contours

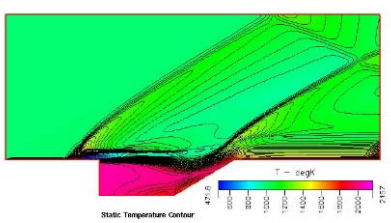

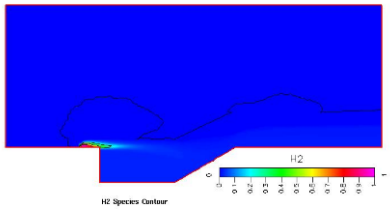

(a) Temperature **(b) H2**

Figure 4. Static temperature and H2 species Contours

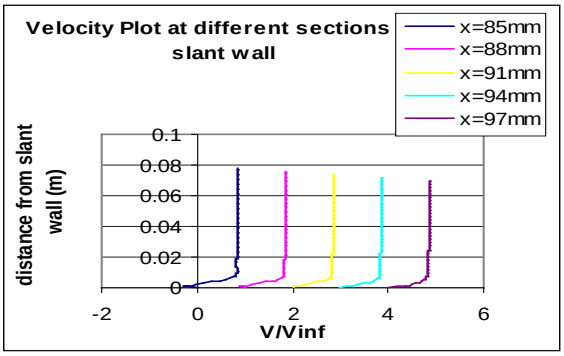

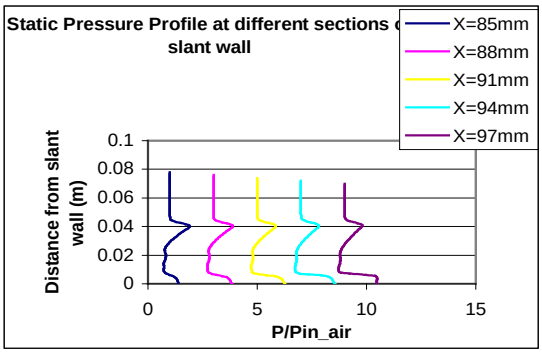

Figure 5. Velocity and static pressure profiles at different section on the slant wall

(a) Static pressure

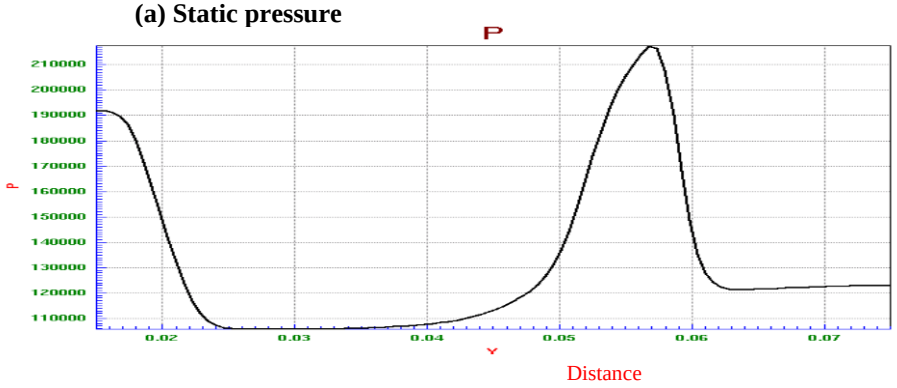

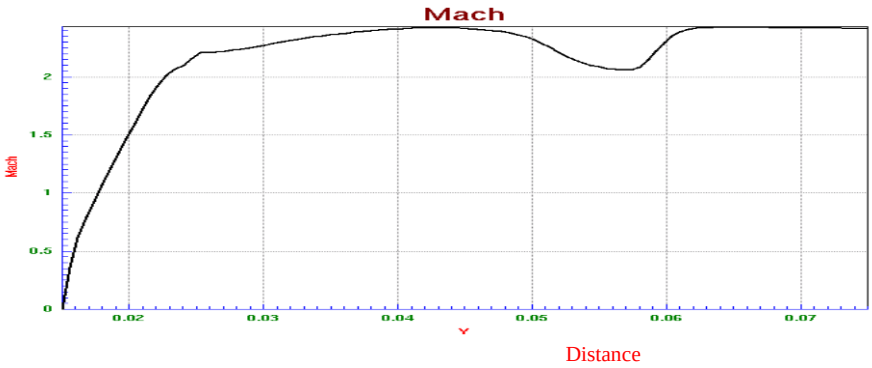

(b) Mach number

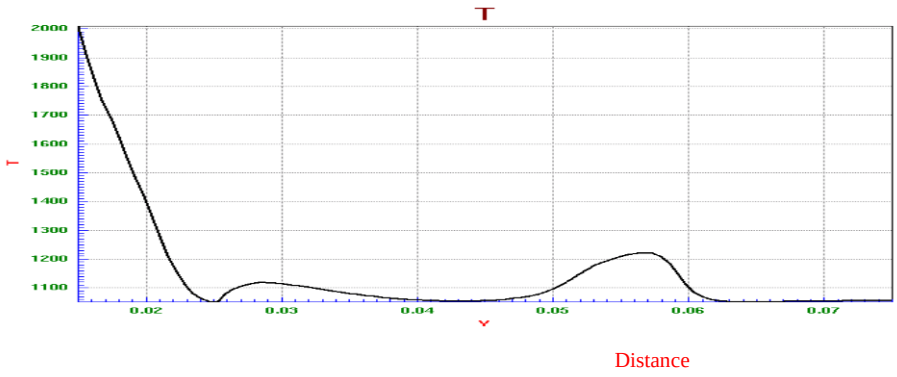

(c) Temperature

Figure 6. Pressure, Mach number and temperature profiles at the exit.

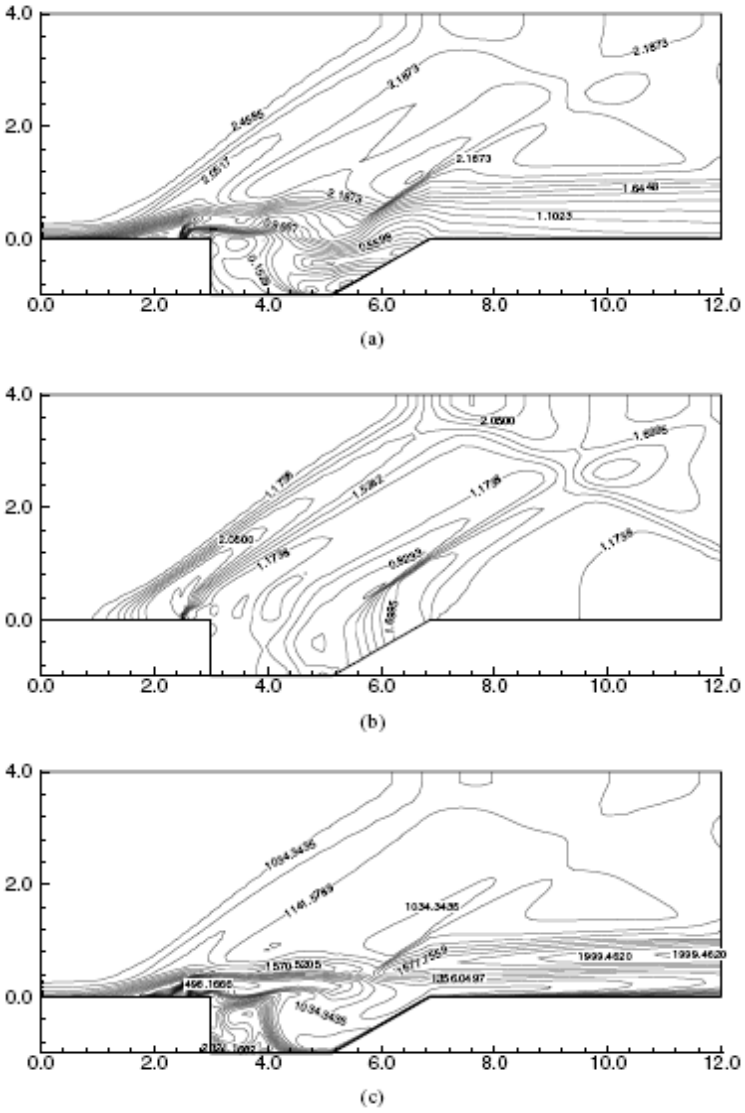

Figure 7. Results from Reference [7] reproduced here for comparison (a) Mach number, (b) Static pressure and (c) Static temperature contours